PROCESS–RESPONSE MODELING OF WAVE-DOMINATED COASTAL SYSTEMS: SIMULATING EVOLUTION AND STRATIGRAPHY ON GEOLOGICAL TIMESCALES

JOEP E.A. STORMS, G.J. WELTJE, J.J. VAN DIJKE, C.R. GEEL, AND S.B. KROONENBERG
Delft University of Technology, Department of Applied Earth Sciences, P.O. Box 5028, NL-2600 GA Delft, The Netherlands
e-mail: j.e.a.storms@ta.tudelft.nl

ABSTRACT: **Numerical modeling on a geological timescale is a rapidly expanding tool to investigate controls on formation of the stratigraphic record. Modeling enables us to test existing ideas, but verification of model results is commonly difficult. Many models are based on geometric or diffusion rules, yet neither type of model has much relevance with actual processes that control sedimentary systems.**

Here we describe a process–response approach to model the evolution and stratigraphy of wave-dominated coastal systems in two dimensions, based on simple approximations of cross-shore erosion and sedimentation. Separating erosion and deposition functions enables us to simulate coastal evolution, stratigraphy, erosion surfaces, and transport of multiple-grain-size classes. The simulated stratigraphic record contains detailed information on grain size and stratal geometry.

We calibrated the model with data sets on coastal transgression in the Caspian Sea, Dagestan, and on grain-size distributions at the island of Terschelling, The Netherlands. Furthermore, hypothetical examples are presented to show the effect of changes in sea level and sediment supply, substrate slope, and sediment size distribution. These tests show that the model is capable of reproducing widely accepted conceptual models of coastal evolution on geological timescales (progradation, aggradation, and various modes of retrogradation).

INTRODUCTION

The complex interaction between variables such as wave climate, sea level, sediment budget, offshore and onshore slopes, and local morphology results in specific coastal behavior and stratigraphic records along sandy shore-zone systems. Coastline migration (retrogradation, aggradation, or progradation) is constrained by the ratio of accommodation to sediment supply and controls the preservation potential of coastal sediments. Swift et al. (1991) described the long-term uniformity of the processes acting in the coastal area in terms of a sediment source area and dispersal systems. Sediment originating from the upper shoreface (source area) is redistributed via several dispersal systems: shoreface, backbarrier/lagoon, and tidal system, if present. Grain size and rates of deposition decrease away from the proximal part of the dispersal system towards the distal parts. This definition of source area and dispersal systems, however, does not specify the processes responsible for erosion and deposition, which can be described on various temporal and spatial scales. Many case studies of coastal processes and evolution exist for the Holocene (e.g., Swift 1975; Thom 1983; Heron et al. 1984; Penland et al. 1985; Davis 1994; Forbes et al. 1995), and although many of these authors stress that local coastal development is unique, the long-term effects of processes responsible for coastal evolution are recognized to be relatively uniform. Numerical modeling can therefore be used to test and integrate these ideas of long-term evolution.

There are many different approaches to numerical modeling, with each approach best suited to specific goals. For example, many two-dimensional and three-dimensional models have been developed to simulate coastal changes on time scales of interest to civil engineers (10^0–10^2 y). Such models are based on well-understood hydrodynamic processes, but their complexity does not allow them to be applied to geological time scales ($> 10^3$ y). Geometric models and diffusion models have been developed to overcome this problem. Bruun (1962) proposed an empirical two-dimensional geometric formulation for the description of equilibrium shoreface profiles. Many others have used or adapted the so-called ''Bruun rule'' or have used similar geometric rules to describe profile shapes (e.g., George and Hand 1977; Cant 1991; Cowell et al. 1999; Pilkey and Davis 1987; Stive and de Vriend 1995; Dubois 1990; Nummedal et al. 1993a; Steckler 1999). In this approach, shoreline migration is calculated by moving the predefined profile in accordance with an imposed sea-level curve and sediment supply, which quantifies and visualizes the existing ideas of shoreface translation and provides insight into the preservation potential of coastal deposits as long as the assumed geometric rules are valid. The validity of geometric rules over the long term, however, is not clear, and there is no feedback between geometry and coastal evolution in the model. In contrast to geometric models, diffusion models (e.g., Kaufman et al. 1992; Niedoroda et al. 1995) produce equilibrium profiles that depend on the imposed parameter setting (diffusion constant, sediment budget, sea-level change). They are often used because of their simplicity and wide applicability to different sedimentary systems. The drawback of diffusion models is the difficulty of modeling transport of multiple grain-size classes. Some diffusion models provide information on sedimentary facies based on the distance between a deposit and its source, but these arbitrary facies do not incorporate lithological information.

Many geological coastal simulation models have sought to simulate shoreface translation or a stratigraphic record that can be viewed and interpreted in a sequence-stratigraphic framework. A combination of shoreface translation and the resultant stratigraphic record (including grain-size information) would be preferable, however, because the two are closely connected. A simulated stratigraphic record will not be correct if the rates and style of shoreface translation are not plausible, and vice versa. Although many existing models are two-dimensional, coastlines are essentially three-dimensional features with along-shore variation of the coastline in the form of spits, bars, or occasional tidal inlets that influence both along-shore and cross-shore erosion and deposition patterns. Therefore, two-dimensional models simplify reality more than three-dimensional models but are relatively easy to use whereas runtime is fast. This has advantages over a complex and time-consuming three-dimensional model if used only as a research tool to better understand basic coastal evolution and the resultant stratigraphic record.

In this paper we describe a two-dimensional model that relates coastal evolution to the depositional record. We model long-term evolution of the system by a process–response approach (Hardy and Waltham 1992; Storms et al. 1999) that simulates the dynamic behavior of a wave-dominated coastal system through the interaction between erosion and deposition. The combination of erosion, deposition, and initial substrate slope results in a unique morphology that ranges from a cliff coast (very high substrate slope) to a barrier-type coast (gentle substrate slope), and a dynamic equilibrium in form is maintained by feedback between shoreface processes. In other words, the shoreface profile will adapt only if the sea level or the sediment supply changes. Separating erosion and deposition enables us to simulate multiple grain-size classes and erosion surfaces, and in doing so the model produces geometry and grain-size data for potential reservoir and aquifer sand bodies that can be used as input for flow simulators. It can help to interpret and connect subsurface data and observations made on outcrops. The model can be run on modern PCs, and calculation time is on the order of a minute per run.

JOURNAL OF SEDIMENTARY RESEARCH, VOL. 72, NO. 2, MARCH, 2002, P. 226–239
 1527-1401/02/072-226/$03.00

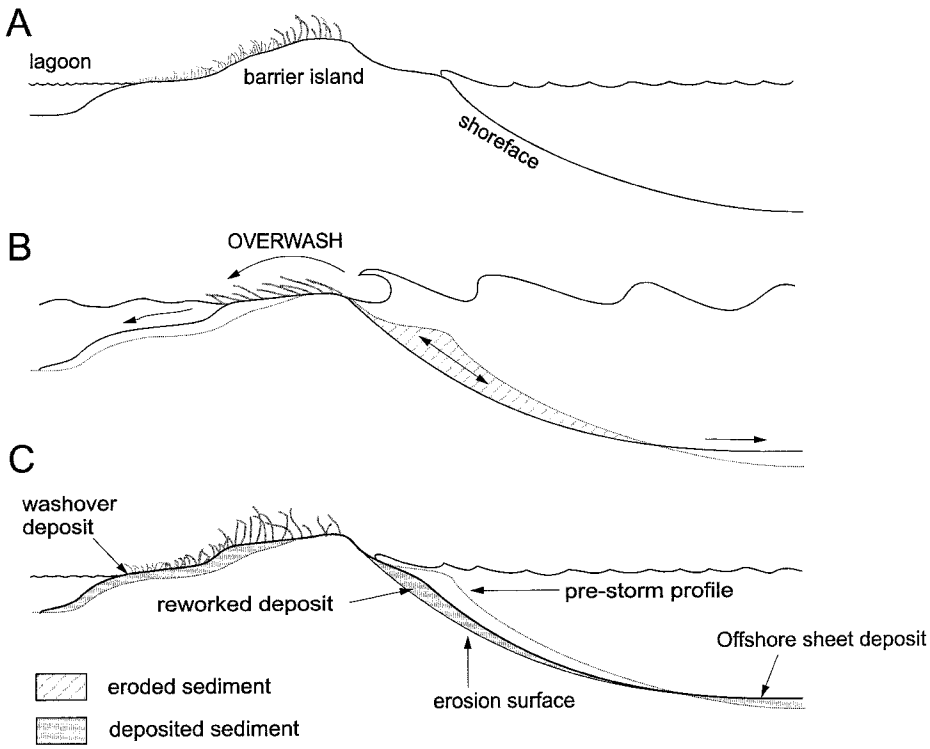

FIG. 1.—Coastal changes after the passage of a large storm. **A)** The pre-storm profile. **B)** The sediment transport directions (arrows) during the storm surge. **C)** The resulting reworked deposits immediately after the storm has passed. The net gain of sediment offshore and in the backbarrier results in a net loss of sediment at the shoreface. Part of the offshore deposits returns landward because of wave action. Redrawn after Penland et al. (1985).

CONTROLS ON COASTAL EVOLUTION

Cross-shore processes driven by wave energy govern the evolution of wave-dominated coastal systems (Davis and Hayes 1984). The available wave energy determines the adaptability of the coastline to changes in sea level and sediment supply. The coastal system tends towards an equilibrium profile, and the amount of energy available to the coast determines the rate at which a new equilibrium is reached under changing external factors (sea level and sediment supply). This results in commonly observed coastal evolution patterns such as retrogradation, aggradation, and progradation (Curray 1964). The offshore slope plays an important role in determining the coastal type (Roy et al. 1994; Kaplin and Selivanov 1995) and influences the rate of retrogradation or progradation. The slope of the upper shoreface and beach, which is related to the grain size of the sediment (Carter 1988; Swift 1975), determines the effectiveness of the wave power, and whether the coast is reflective, dissipative, or intermediate (Wright and Short 1983).

Penland et al. (1985) illustrated that the majority of changes along a sediment-starved intermediate wave-dominated barrier coast occur during storm events (Fig. 1), because high-energy storm passage produces severe scouring of the shoreface to storm wave base depth. We define storm wave base as the maximum seaward location for resuspension of unconsolidated sediment by wave action during a storm. The location of the storm wave base constantly changes because each storm has a characteristic wave spectrum. Wave-generated bottom currents transport grains as traction load or suspended load, depending on the flow velocity and grain size of the sediment. The mobilized sediment may be transported to the backbarrier by washover (e.g., Leatherman and Williams 1983), or it may be either redeposited at the shoreface or passed on to deeper water beyond the storm wave base (Swift and Thorne 1991).

Swift and Thorne (1991) described a decreasing grain size in both shoreface and backbarrier deposits away from the coastline. Washover deposits are also characterized by a fining trend towards the lagoon (Leatherman and Williams 1983). At the shoreface, the interaction between the hydraulic regime and the available sediment generates a spatial equilibrium distribution of grain-size fractions (Guillén and Hoekstra 1996), which can be regarded as a fingerprint of the system. For example, a shoreface nourishment project at Terschelling, the Netherlands, showed that the equilibrium distribution was reestablished within six months after introducing a considerable amount of relatively coarse-grained sediment to the upper shoreface (Guillén and Hoekstra 1996 1997). Hence the system responds instantaneously on a geologic time scale.

Some assumptions need to be addressed prior to the modeling. Local variations over short time scales (such as channels due to rip currents, nearshore bars, or beach cusps) are assumed to have little significant effect over longer time scales. No eolian processes are modeled. We assume for simplicity that the subaerial part of the barrier acts as a temporary storage of sediment. Subaerial parts of the barrier have a local effect on washover by blocking the washover flow. However, washovers can always reach the backbarrier because barrier islands are discontinuous along-shore. The simulated cross profiles should therefore be regarded as spatially averaged.

PROCESS–RESPONSE MODEL OF COASTAL EVOLUTION

Our model of coastal evolution is based on the continuity equation:

$$\frac{\partial H}{\partial t} = -\frac{\partial F}{\partial x} + T \tag{1}$$

where t is time [T], x is horizontal distance [L], H is topographic elevation relative to a constant reference level [L], F is sediment flux [$L^2\ T^{-1}$] and T is rate of subsidence due to the combined effects of compaction, loading, and vertical movements of the basin floor [$L\ T^{-1}$]. The spatial derivative of the sediment flux is defined as the difference between rates of erosion and rates of deposition:

$$\frac{\partial F}{\partial x} = E(x, t) - S(x, t) \tag{2}$$

where $E(x,t)$ is the rate of erosion [L T^{-1}] and $S(x,t)$ is the rate of deposition [L T^{-1}].

Erosion

We define the rate of erosion as

$$E(x,t) = c_e G(x,t) \tag{3}$$

where c_e is the maximum coastal erosion rate [L T^{-1}] and $G(x,t)$ is the local erosion efficiency [-].

Location $x_s(t)$ corresponds to the coastline, which is defined by the intersection of sea level $H_s(t)$ and the topographic profile. Erosion is limited to a shoreface erosion window defined by the spatial domain between locations $x_c(t)$ and $x_w(t)$, and outside of this domain, $E(x,t)$ is taken to be zero. Location $x_c(t)$ is defined as the landward boundary of the shoreface erosion window: $x_c(t) = x_s(t) - \Delta x_e$, where Δx_e represents the maximum horizontal extent of inland erosion by wave energy. The topographic elevation at $x_c(t)$ is defined as $H_c(t)$. Location $x_w(t)$ is defined by the intersection of the storm wave base $H_w(t)$ and the topographic profile. The storm wave base $H_w(t)$ is defined by: $H_w(t) = H_s(t) + z_w$, where z_w is the storm wave base [L]. The storm wave base is related to storm recurrence interval, because small storms occur more often than large storms and should therefore be adjusted according to the timestep used in the model.

The above definitions allow us to formulate local erosion efficiency, with values ranging from unity in the vicinity of the coastline to zero at the storm wave base:

$$G(x,\,t) = \begin{cases} \left(\dfrac{\max[H_w(t),\,H(x,\,t)] - H_w(t)}{H_c(t) - H_w(t)}\right)^m \\ \quad \text{for } x_c(t) < x < x_w(t) \\ 0 \quad \text{for } x \le x_c(t) \quad \text{and} \quad x \ge x_w(t) \end{cases} \tag{4}$$

where m is a constant [-] that represents the dependence of erosion rate on water depth. We have set $m = 3$ in our simulations. Note that erosion efficiency is independent of the properties of the substrate, which is assumed to consist of unconsolidated sediment.

Deposition

The deposition function used in the model is given by

$$S(x,\,t) = \frac{F(x,\,t)}{h} \tag{5}$$

where F is the flux of sediment that is in transit, available for deposition [L^2 T^{-1}]. The flux of available sediment is defined as the sum of local influx plus material eroded from the bed. The deposition algorithm partitions this flux of locally available sediment into a local deposition flux and a local outflux:

$$F = F_{in} + F_{ero} = F_{dep} + F_{out} \tag{6}$$

h represents the sediment travel distance [L], which depends on the grain size of the sediment and on the environment of deposition (i.e., the flow properties of the transporting medium). The net effects of size-selective transport are simulated by the size dependence of the travel distance h in the deposition function. Cross-shore sediment dispersal is described by the following relationship between the nominal grain diameter D [mm] and h [m], for a standard spatial increment of 50 m as

$$h^*(D) = \begin{cases} c_h\left[110 + 590\left(\dfrac{D_{ref}}{D}\right)^{2.5}\right] & \text{for } D > D_{ref} \\ c_h\left[500 + 200\left(\dfrac{D_{ref}}{D}\right)^{0.6}\right] & \text{for } D \le D_{ref} \end{cases} \tag{7}$$

where $D_{ref} = 0.125$ mm. The dominant mode of transport in fully turbulent unidirectional flows of sediments below this size is in suspension, whereas sediments above this size are transported mostly as traction load (Bridge 1981; Bridge and Bennett 1992). The constant c_h accounts for the variability in local conditions [-]. The relationship between the nominal grain diameter D and h is based on data from Terschelling, the Netherlands (Guillén and Hoekstra 1996, 1997) and will be discussed below in the calibration section.

The inverse of travel distance, h^{-1}, is proportional to the probability of deposition along a transport pathway of a fixed length, implying that travel distances can vary with changes of grid size. The following transformation of travel distance allows one to retain the same depositional geometry with grid sizes other than 50 m:

$$\begin{aligned} \tilde{h}(D) &= h^*(D) && \text{if } \Delta x = 50 \\ \tilde{h}(D) &= \frac{\Delta x}{\left\{1 - \left(1 - \dfrac{50}{h^*(D)}\right)^{0.02\Delta x}\right\}} && \text{if } \Delta x \ne 50 \end{aligned} \tag{8}$$

Note that the smallest travel distance should always exceed the grid size to ensure that the probability of deposition remains less than one. Sediments whose travel distance equals or exceeds the grid spacing cannot be transported to another cell.

Our model simulates wave-driven sediment transport in both the landward and the seaward cross-shore direction, but it does not include eolian processes or infilling of the lagoon by fine-grained material originating from inland fluvial sources. In reality, wave-driven deposition can occur above mean sea level as a result of storm surge and wave setup, forming washover channels and lobes. In the model, however, most sediment bypasses washover channels to be deposited in the backbarrier and bypassing is incorporated by the dependence of travel distance on water depth:

$$h(z,\,D) = \tilde{h}(1 + e^{Az}), \tag{9}$$

where

$$z = \frac{H(x,\,t) - H_s(t)}{z_l}$$

The depth dependence of travel distance implies that relative deposition fluxes begin to decrease at a depth of z_l below sea level. Relative deposition fluxes at sea level are exactly half of unconstrained deep-water fluxes, and they are effectively zero at z_l above sea level. We have set $A = 6$ and $z_l = 0.5$ m in most simulations.

Erosion is defined between the shoreline and the storm wave base, but deposition may take place in the backbarrier and seaward of the storm wave base, and therefore the model is not a closed system. However, coastal regression and transgression may result in erosion of this sediment at a later stage during the simulation. Furthermore, sediment introduced to or removed from the coastal system by littoral drift may play an important role. Littoral drift cannot be directly incorporated into a two-dimensional model, hence we simulate it by varying influx. Rates of sediment influx used in this paper vary between 0 and 10 m^2/y.

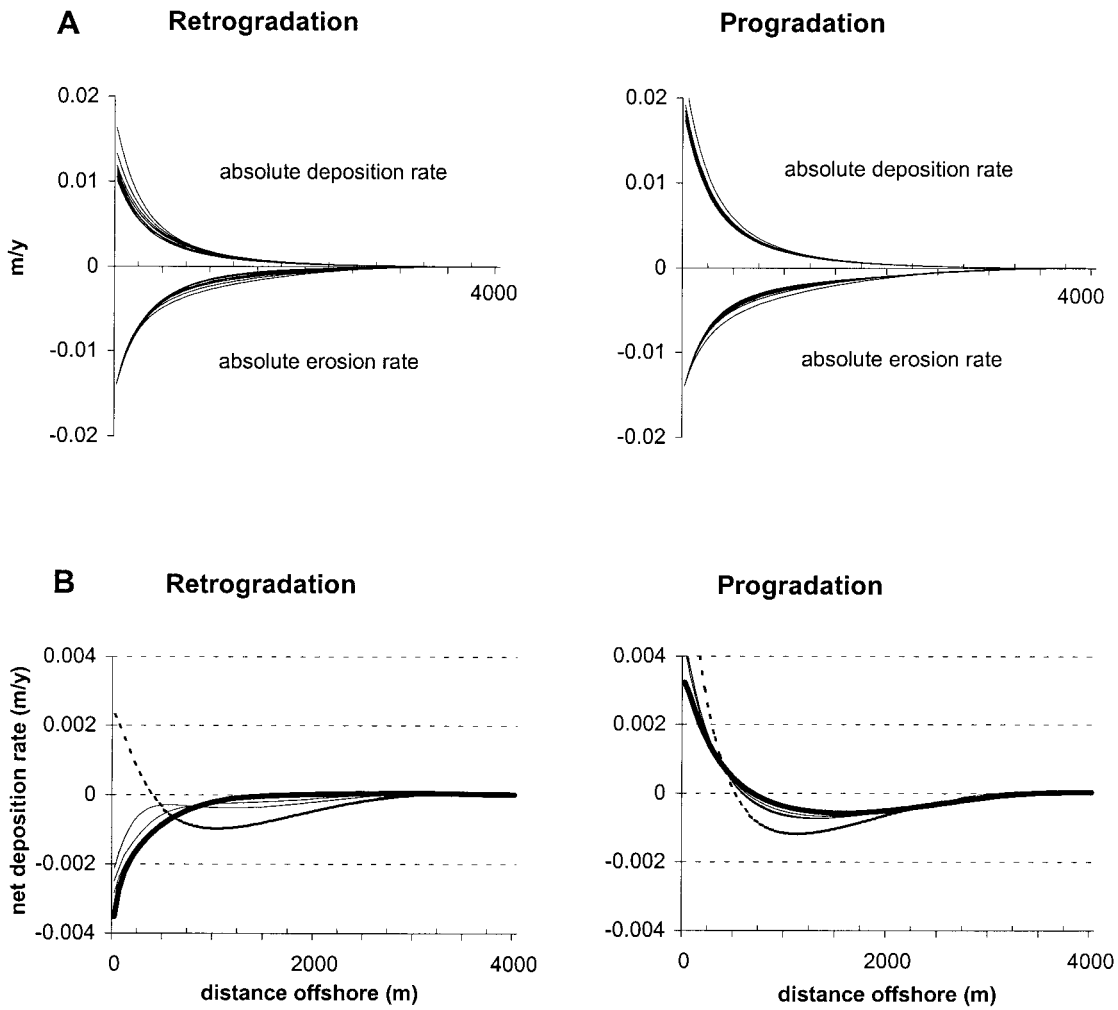

FIG. 2.—**A)** Simulated shoreface erosion and deposition rates relative to the shoreline position during retrogradation and progradation (forced regression). Each thin line represents a timestep. **B)** Simulated net shoreface erosion or deposition rate relative to the shoreline position based on part A). The dotted line represents the first timestep; the bold line represents the last timestep. The intermediate lines illustrate individual timesteps. It takes some time to reach equilibrium conditions in the retrogradation case. See text for further explanation.

MODEL VARIABLES

A distinction can be made between model parameters, time-dependent variables, and initial conditions. Model parameters are used to tune the model, and they consist of characteristic travel distances for each defined grain-size class *h(D)*, rate of erosion, c_e,and wave efficiency c_h. Time-dependent variables are sea level and sediment budget. Initial conditions are the grain-size distributions of the substrate and of the sediment that is added or removed by littoral drift, wavebase depth, and substrate slope. Substrate slope is the regional slope of underlying deposits stretching from the shelf edge to the inland areas. The shoreface form represents a dynamic equilibrium between erosion and deposition, which is fully adapted to substrate slope, grain size of the sediment, and rates of sea-level change and sediment supply.

Figure 2A shows the distribution of erosion and deposition at the shoreface for a hypothetical retrogradational and a progradational case over a 50-year interval. The regional substrate slope for both cases was set to 0.14°, which results in a typical simulated barrier profile. A linear sea-level rise and fall of 0.0012 m/y was imposed to simulate retrogradation and progradation, respectively (Fig. 2A). Progradation resulting from sea-level fall is called forced regression, whereas progradation originating from high sediment supply during a stable or rising sea level is called normal regression (Posamentier et al. 1992; Plint 1988; Nummedal et al. 1993b). In our case the progradation is a direct result of the sea-level fall. The initial grain-size distribution was identical in both cases. All changes are due to reworking, because no additional sediment was introduced to the systems by littoral drift. The erodibility parameter c_e was 0.014 m/yr in both cases (equivalent to a maximum reworking depth of the sediment column at the coastline of 0.7 m for $\Delta t = 50$ y and decreasing seaward; see lower part of Fig. 2A).

The upper part of Figure 2A shows the differences in absolute rate of deposition. The shape of the curves is the same because the sediment travel distances are similar for both cases, but the deposition rate for the progradational case is higher. This is explained by the loss of shoreface sediment due to washover in the retrogradational case. Figure 2B shows the net deposition rate as the difference between erosion and deposition. The dotted line indicates the first timestep, when equilibrium conditions are not yet achieved, whereas the bold line indicates the last timestep, discussed below. In the retrogradational case a maximum net vertical erosion rate of 3.4 m/ky is recorded between the coastline and about 1750 m offshore. Beyond 1750 m net deposition takes place at a maximum rate of 0.054 m/ky at 3000 m offshore. This suggests that upper and middle shoreface deposits ($<$ 1750 m offshore) are not preserved during retrogradation, in contrast

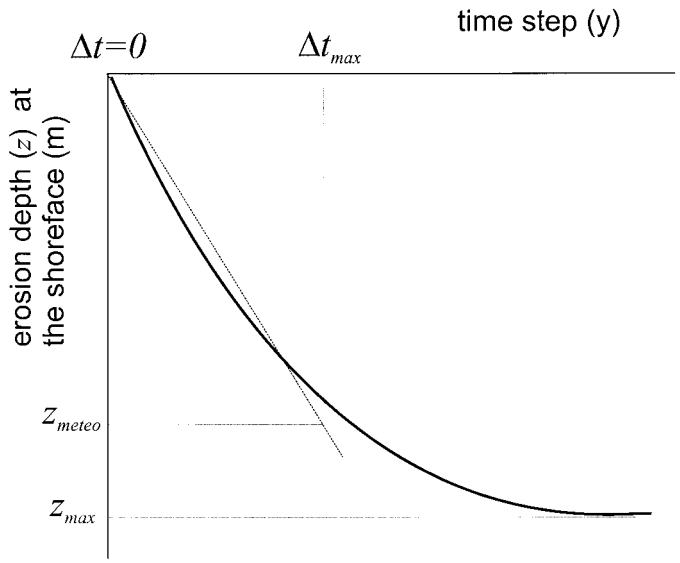

FIG. 3.—Supposed relationship between absolute shoreface erosion depth z and timestep Δt. See text for explanation. The model assumes a linear relationship between timestep and absolute erosion rate and is therefore applicable only for timesteps smaller than Δt_{max}.

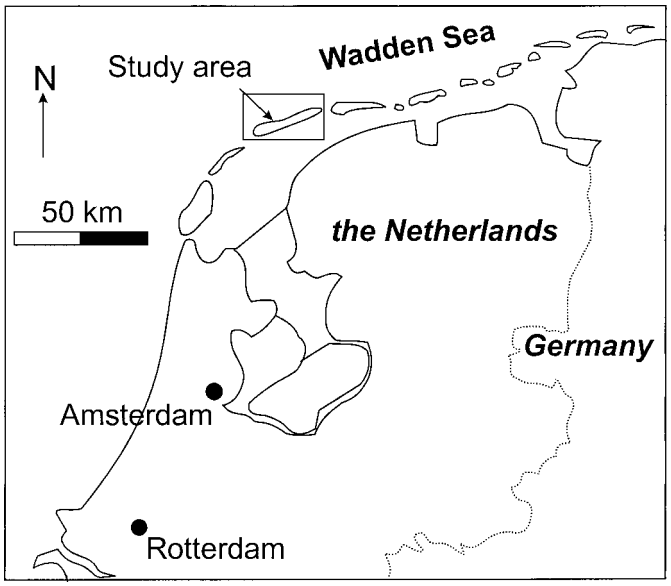

FIG. 4.—Location map of Terschelling, the Netherlands. The sediment grain-size samples are taken at the seaward side of the barrier island indicated by the box.

to lower shoreface deposits. The progradational case tells a different tale (Fig. 2B). Here net deposition takes place at the upper shoreface ($<$ 650 m offshore) and net erosion at the middle and lower shoreface between 650 m and about 3450 m offshore. Beyond 3450 m net deposition takes place at a very low rate ($<$ 0.03 m/ky). However, the lower shoreface deposits are eroded because the whole system progrades owing to the sea-level fall, and only upper shoreface deposits are preserved. This suggests that in general, during retrogradation, only relatively fine-grained lower shoreface deposits are preserved whereas during progradation only relatively coarse-grained upper shoreface deposits are preserved (Fig. 2B).

The choice of time increments in the model is constrained by our formulation. Figure 3 shows the assumed relationship between timestep and absolute erosion depth (or reworking depth) at the shoreface. By using a fixed rate of erosion, c_e, it is assumed that a linear relationship exists between time interval and erosion depth, as represented by the straight line in Figure 3. One can assume, however, that storm magnitude has a meteorologically restricted maximum that is applicable to large ($\sim 10^3$ y) timesteps (Fig. 3). This implies that the maximum timestep used by the model is restricted. The slope of the dotted line in Figure 3 is related to the wave-efficiency parameter c_h which accounts for the variability in local conditions.

CALIBRATION

We used data on modern shoreface grain-size distributions from Terschelling, the Netherlands (Guillén and Hoekstra 1996, 1997) to calibrate the relationship between grain size and sediment travel distances used in the model. Additionally, we compared model results against data derived from monitoring the response of a coastal barrier system along the Caspian Sea in Dagestan to a rapid local sea-level rise of 2.5 m in 20 years (Kroonenberg et al. 2000).

Sediment Grain-Size Distribution

Guillén and Hoekstra (1996, 1997) collected 180 sediment samples from seven cross-shore profiles along the Terschelling coast. The island of Terschelling is one of the seven largest West Frisian barrier islands, with a length of about 27 km (Fig. 4). The samples were collected between the dune foot and approximately 1900 m offshore. All samples were sieved into 16 grain-size classes between 100 and 475 μm, and the weight percentages of the fractions were calculated for each sample. Grain-size distributions and shoreface morphology are similar for all seven cross-shore profiles.

The initial grain-size distribution used in the calibration model run was determined by averaging across all sediment samples. Figure 5A shows the Terschelling grain-size distribution, for which sediment becomes both finer and better sorted in an offshore direction. This agrees well with the progressive sorting trend described by Swift and Thorne (1991), among others. Figure 5B shows the simulation results using best-fit travel distances. Comparison between Figure 5A and 5B shows that the grain-size distribution is accurately matched, whereas Figure 6 shows that the simulated equilibrium shoreface fits the Terschelling data points well.

Coastal Dynamics

In order to test coastline evolution simulated by the model we used a 20-year monitoring data set of the Dagestan Coast along the Caspian Sea (Fig. 7). The Caspian Sea is a land-locked basin without tidal influence, and its rapidly changing sea level largely reflects the variability in Volga River discharge as a function of secular changes in global climate (Rodionov 1994; Arpe et al. 2000). Figure 8 shows the mean annual sea-level curve and the total coastline retreat for the Caspian Sea between 1977 and 1997. Coastline retreat, island width, and lagoon width and depth were measured on an annual basis. After a lowstand in 1977 sea level began to rise until a highstand was reached in 1995, with a total increase of 2.5 m. Kroonenberg et al. (2000) showed that this period was characterized by development of a transgressive barrier coast (Fig. 8) and erosion of the pre-1977 strandplain. Data on barrier-island width, lagoon width, and lagoon depth is shown in Figure 9A. Between 1977 and 1987, width and depth of the lagoon slowly increased. Island-width data are not available for this period. From 1987 to 1994, however, the width and depth of the lagoon increased while the width of the barrier island actually decreased. After this time the lagoon width decreased and the island width increased again.

We simulated the coastal evolution of the Dagestan coast by using the sea-level curve (Fig. 8) and the 1977 profile as input. We used an ''average storm'' occurring twice a year which corresponds to a storm wave base of

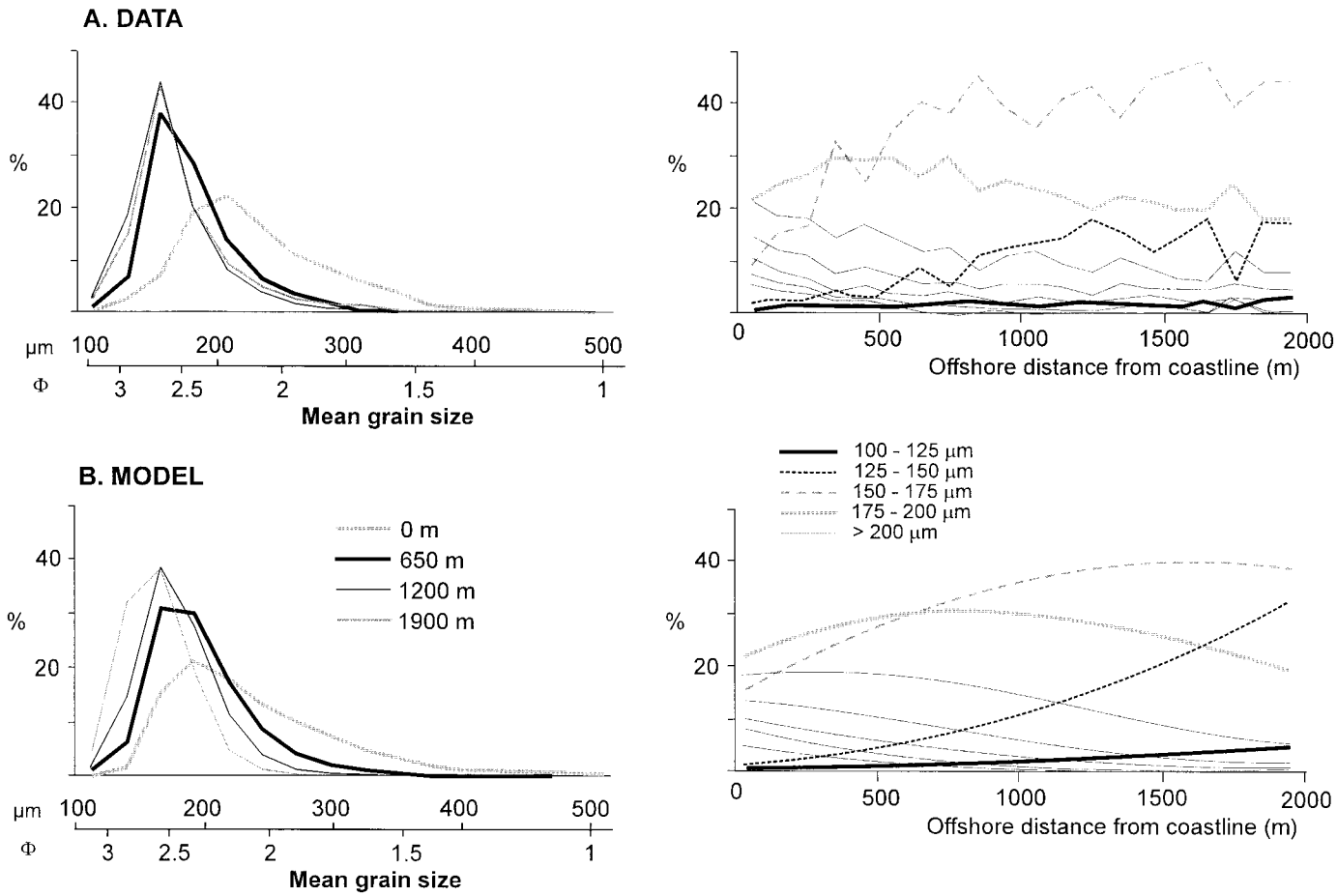

FIG. 5.—**A)** The left-hand side shows the averaged grain-size distribution at the beach and at three offshore locations (650 m, 1200 m, and 1900 m) from the Terschelling shoreface. The right-hand side shows the averaged cross-shore distribution of grain-size classes. The data revealed no significant alongshore variation or trend in the data. Both graphs are based on 180 sediment samples (from Guillén and Hoekstra 1996). For location see Figure 4. **B)** The simulated grain-size distributions.

4 m. It was assumed that no sediment was added to, or removed from, the system. Figure 9B illustrates that the model can reproduce the observed coastal behavior. The lagoonal water level in the model was assumed to be equal to sea level, even though this need not be the case because high precipitation and the absence of inlets can have resulted in an elevation of lagoon level relative to sea level. Further offset between data and model may be explained by the combined action of storms and sea-level changes in the data while the model is driven only by sea-level changes. Trends in coastal behavior are, however, fairly well reproduced.

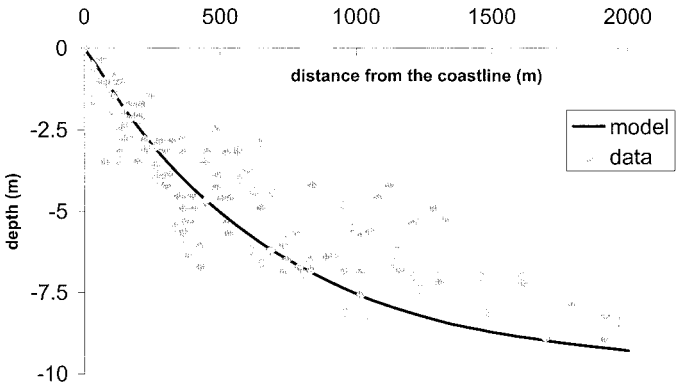

FIG. 6.—Dots illustrate all 180 depth measurements from 7 cross-shore profiles representing the ''average'' Terschelling shoreface profile (from Guillén and Hoekstra 1996). Local bars cause variation in the depth measurements. The solid line shows the simulated shoreface profile. For location see Figure 4.

Applications of the model to real-world data show that the model is capable of simulating spatial patterns of grain-size distributions and basic coastal evolution for Terschelling and the Dagestan coast. This implies that the simplified representation of the dominant processes acting on the coastal system appear to be valid for these cases.

HYPOTHETICAL SCENARIOS

Four hypothetical examples of the effects of substrate slope, grain-size distributions, and rates of sediment supply and sea-level changes are presented to illustrate their influence on coastal morphology and the resulting stratigraphic record. Although the simulated data cannot be directly compared to real-world data, they closely correspond to concepts described in the literature by previous workers. In each example the influence of one parameter on the model output will be highlighted with examples chosen to illustrate the potential applicability of the model. We do not intend to speculate on details of coastal behavior on the basis of these modeling results. Future work will focus on real-world applications such as those discussed below.

Grain Size

Two simulations were carried out with identical settings except for the initial (substrate) sediment grain-size distribution to illustrate the effect of

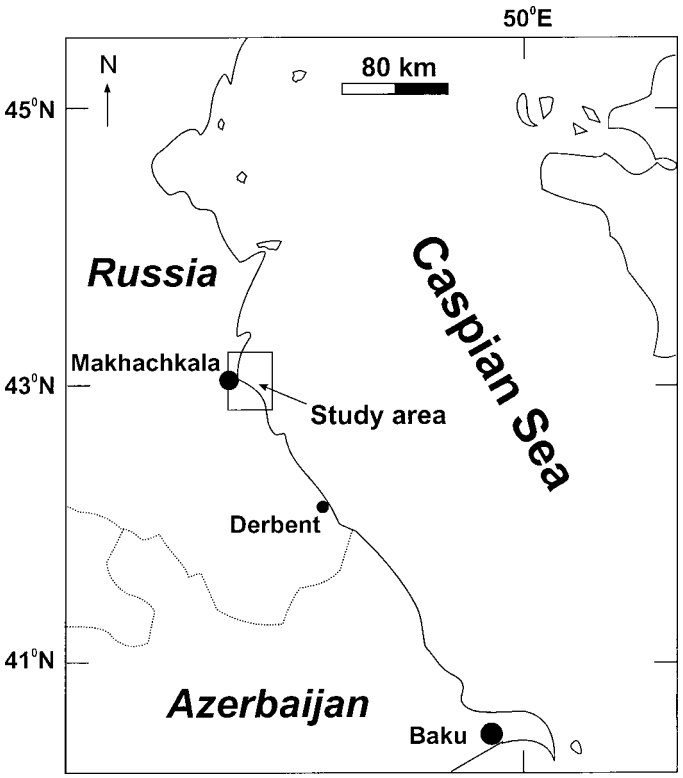

FIG. 7.—Location map of the western Caspian Coast. The Dagestan study site is indicated by the box (Kroonenberg et al. 2000).

source material on coastal morphology. Figure 10 shows two initial grain-size distributions in the range between 100 and 475 μm. Case A represents the relatively fine-grained sediment of the Terschelling shoreface (Guillén and Hoekstra 1996). Case B is the coarse-grained mirror image of case A, considered to be typical for a glacial source. Figure 11 shows the resulting grain-size distribution on the shoreface after reworking. For case A, the sediment becomes finer and better sorted in an offshore direction (Fig. 11). For case B sediment becomes finer in an offshore direction, but the sorting coefficient decreases significantly. These cases illustrate that initial sediment supply and initial grain-size distribution are important in understanding the spatial variation of grain size, because a fining trend in the sediment is not always accompanied by increased sorting.

The coarse sediment in case B results in a steeper shoreface than case

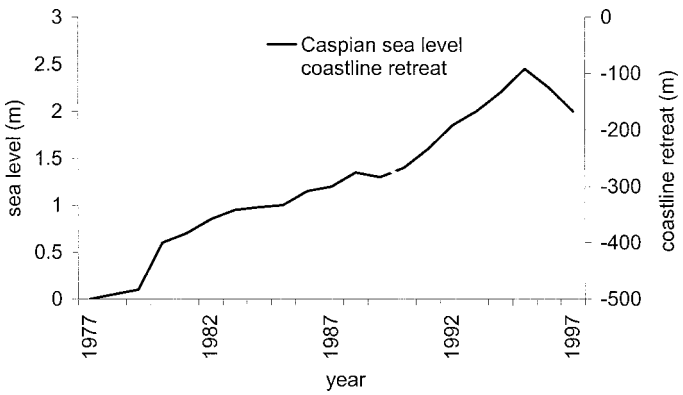

FIG. 8.—Mean annual sea-level curve of the Caspian Sea between 1977 and 1997 (from Polonski et al. 1998) and observed retreat of the Dagestan coastline (Kroonenberg et al. 2000). For location see Figure 7.

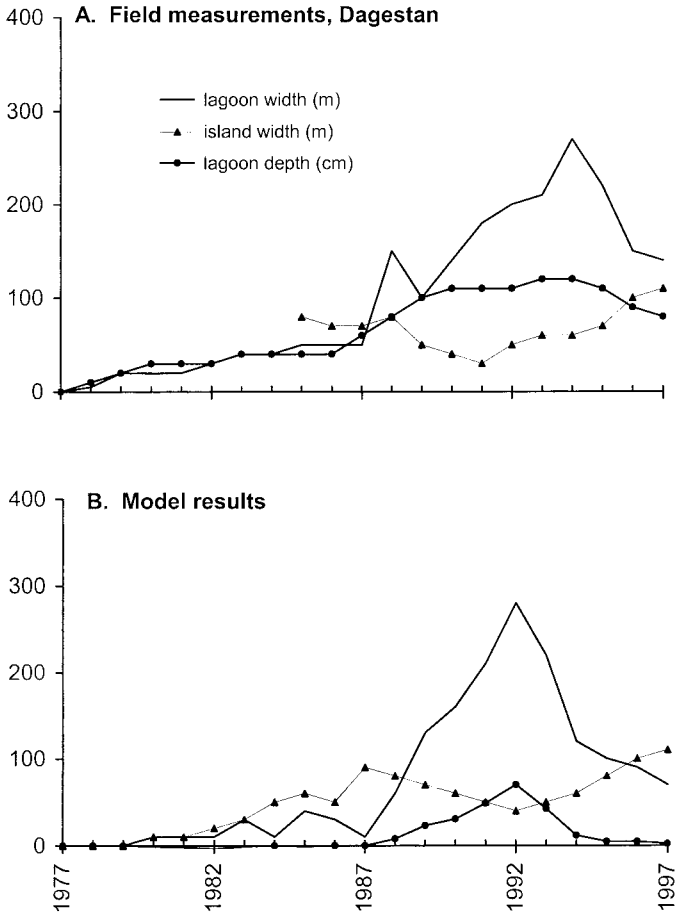

FIG. 9.—**A)** Monitoring data of the transgressive Dagestan coast, Caspian Sea, between 1977 and 1997 (Kroonenberg et al. 2000). **B)** The simulated model results. For location see Figure 7.

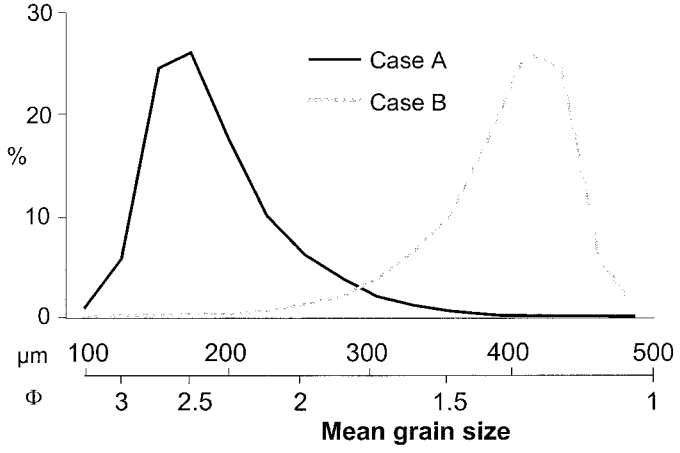

FIG. 10.—Initial sediment grain-size distribution used for two model experiments. Case A represents the sediment grain-size distribution as used for the Terschelling shoreface (Guillén and Hoekstra 1996) simulation. Case B is the coarse-grained mirror image of case A, considered to be typical for a glacial source.

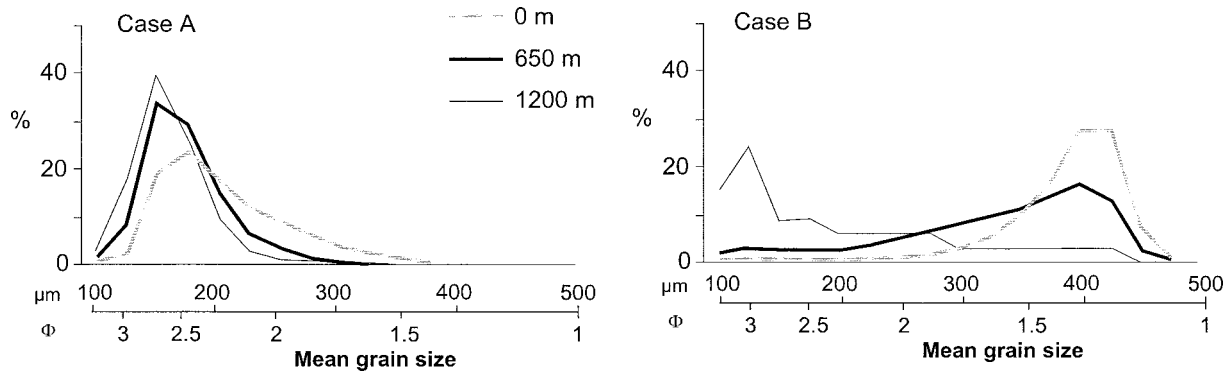

FIG. 11.—Simulated grain-size distributions for cases A and B at 3 shoreface locations based on the initial sediment distribution from Figure 10.

A (Fig. 12). This is the sole effect of the substrate grain-size distribution. The steepest shoreface parts of cases A and B are 0.83° and 1.86° respectively, and can be regarded as the beach-foreshore. Carter (1988) related grain size to beach slope on the basis of laboratory and field data. Slope values for both simulations presented here are within the range that would be expected from Carters' (1988) data, as shown in Figure 13.

Rate of Sediment Supply

Curray (1964) described the interaction of sea-level change and the rate of deposition as the driving force behind regression and transgression of the coastline. Later, Helland-Hansen and Martinsen (1996) described the balance between sea level and sediment supply in more detail in terms of shoreline trajectories. They stressed the importance of transgression and regression for understanding the sedimentary record. The simulation of the Dagestan coast (Fig. 9) shows that the model is capable of simulating coastal evolution in the case of a very rapid sea-level rise with no change in sediment supply.

Below, three simple hypothetical examples are presented for evolution of a barrier-type coast with a linear sea-level rise of 4 m (Fig. 14), but with varying rates of sediment supply. The model was initialized with constant sea level and zero sediment supply until an equilibrium profile developed from the initial straight substrate. These equilibrium profiles are equal for cases C through E in Figure 14. Case C shows a retrograding barrier system, where sediment input is insufficient to compensate for the increase in shoreface accommodation due to the rise in sea level. Washover deposits compensate the increase of accommodation in the backbarrier, and the end result is a coastal plain with no distinct lagoon. In case D sufficient sediment is added to the system to stabilize the position of the shoreline. Aggradation occurs while the accommodation landward of the coastline increases. Sediment supply to the backbarrier by washover is insufficient to balance backbarrier accommodation, and a lagoon starts to develop, separating the barrier island from the mainland at the end of the simulation. Finally, case E shows the simulated profile with a high rate of sediment supply. The coastline progrades by 400 m although the sea level rises 4 meters. Backbarrier accommodation is much larger than the supply of sediment by washover, and a wide lagoon develops.

Few data on long-term behavior of oceanic coasts are available because the Holocene has been a period of sea-level highstand and most evidence of coastal retreat is either eroded or located below sea level. This makes direct calibration difficult. A possible alternative is to compare simulation results to outcrop data in terms of geometry, grain-size distributions, and internal structure. The basic problem with this approach is that time-dependent variables are poorly constrained for most ancient basin fills.

Rate of Sea-Level Rise

Case C (Fig. 14) illustrates the effect of sea-level rise dominating over sediment supply. The resulting coastal system retreats landward without significant geometric changes. This type of transgression (continuous retreat; Swift et al. 1991) is generally accepted as the dominant type of retreat. However, Rampino and Sanders (1980, 1982, 1983) describe a more controversial discontinuous retreat model (see discussions by Swift and Moslow 1982; Leatherman 1983) which assumes that a barrier system may be overstepped if the rate of sea-level rise is fast enough to drown the

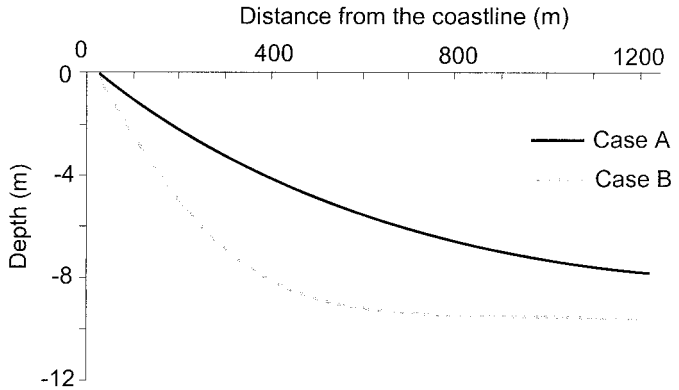

FIG. 12.—Simulated shoreface slopes for cases A and B. Case B reveals a steeper shoreface than case A because of the difference in grain-size distribution.

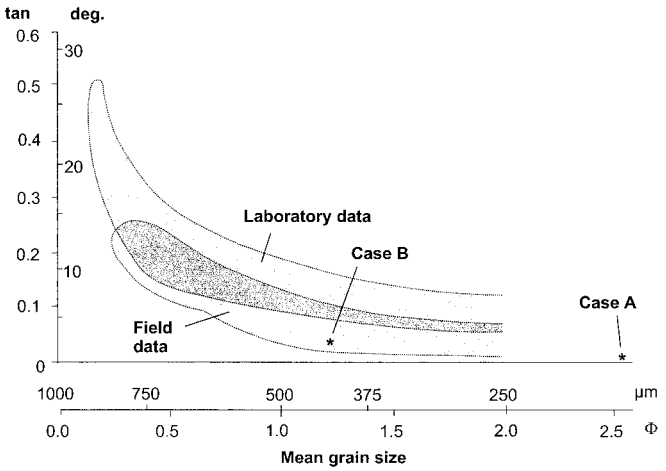

FIG. 13.—Relationship between grain size and beach slope (redrawn from Carter 1988). Simulation results for cases A and B are plotted.

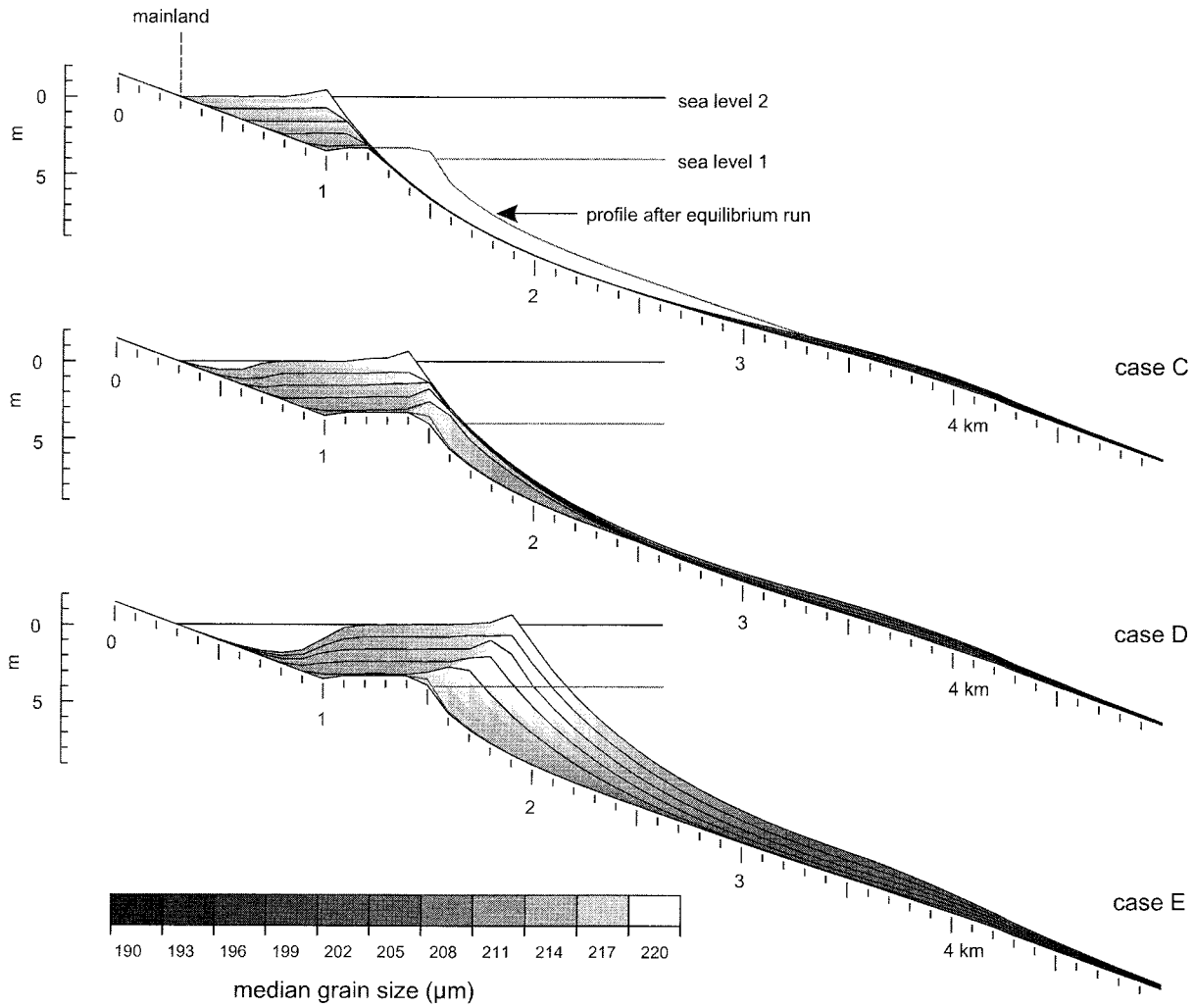

FIG. 14.—Simulated retrogradation (case C), aggradation (case D), and progradation (case E). Sea-level rise for all cases is 4 m. Sediment supply increases from case C to case E. The thin lines indicate time-equivalent lines. Mean grain size decreases slightly from white to dark gray. The horizontal scale is in kilometers; the vertical scale is in meters.

complete barrier in place while the shoreline steps landward. Rampino and Sanders (1980) lend credence to their theory by identification of offshore lagoonal deposits and bars, but they were not the first to describe the overstepping theory. Curray (1964) and Swift (1968) described a mechanism whereby barriers tend to grow upward during transgression until their enlarged lagoons trap so much sediment that the barrier is overstepped. Shoreface reworking generally destroys all evidence of the mode of retreat, thus leaving little evidence for the discontinuous retreat model. However, Forbes et al. (1991) illustrated barrier overstep for gravel barriers.

Two simulations (Fig. 15) have been carried out to illustrate the effect of the rate of sea-level rise on coastal retreat. The total amount of sediment added to the systems is equal in both cases. Case F shows a retrogradational barrier system during a sea-level rise of 0.825 m/ky. Retrogradation is continuous and the width of the barrier island and lagoon reach equilibrium values (see Figure 16). By contrast, case G (Fig. 15) shows the evolution of a barrier system for a faster rate of sea-level rise (3.3 m/ky). In Figure 16 it can be seen that the barrier island becomes narrower, because the landward side of the island retreats at a lower rate than the shoreline. This is explained by the passive deepening and widening of the lagoon as a result of the fast sea-level rise combined with sediment shortage in the backbarrier. Sediment transported to the backbarrier by washover processes is insufficient to compensate for the increase of backbarrier accommodation. As a result, the rate of land loss at the coastline exceeds the rate of land gain by washover on the backbarrier side of the island, the island narrows, and it becomes more and more isolated from the mainland. After about 4000 years the barrier island is at its narrowest and is overstepped. A new island develops at the mainland–lagoon intersection while the drowned barrier is eroded by wave action. The availability of large amounts of sediment on the shoreface from the drowned barrier results in a fast but temporary progradation of the newly formed coastline (Fig. 16). Once the greater part of the drowned barrier is reworked progradation ends and retrogradation is resumed.

Case G (Figs. 15, 16) illustrates an example that may represent a mechanism for barrier overstepping as already described by Curray (1964) and Swift (1968). Several factors besides rate of sea-level change such as sediment supply, substrate slope, and sediment type and erodibility, further influence the mode of coastal retreat. Figure 15 shows that at the shoreface of both cases F and G washover and lagoonal deposits are found (landward dipping timelines). The momentary prograding coast that formed after overstepping consists of relatively coarse sediments. Subsequent retrogradation most probably will erode the major part of this coarse-grained sediment body. Preservation potential of the drowned barrier in this case is small.

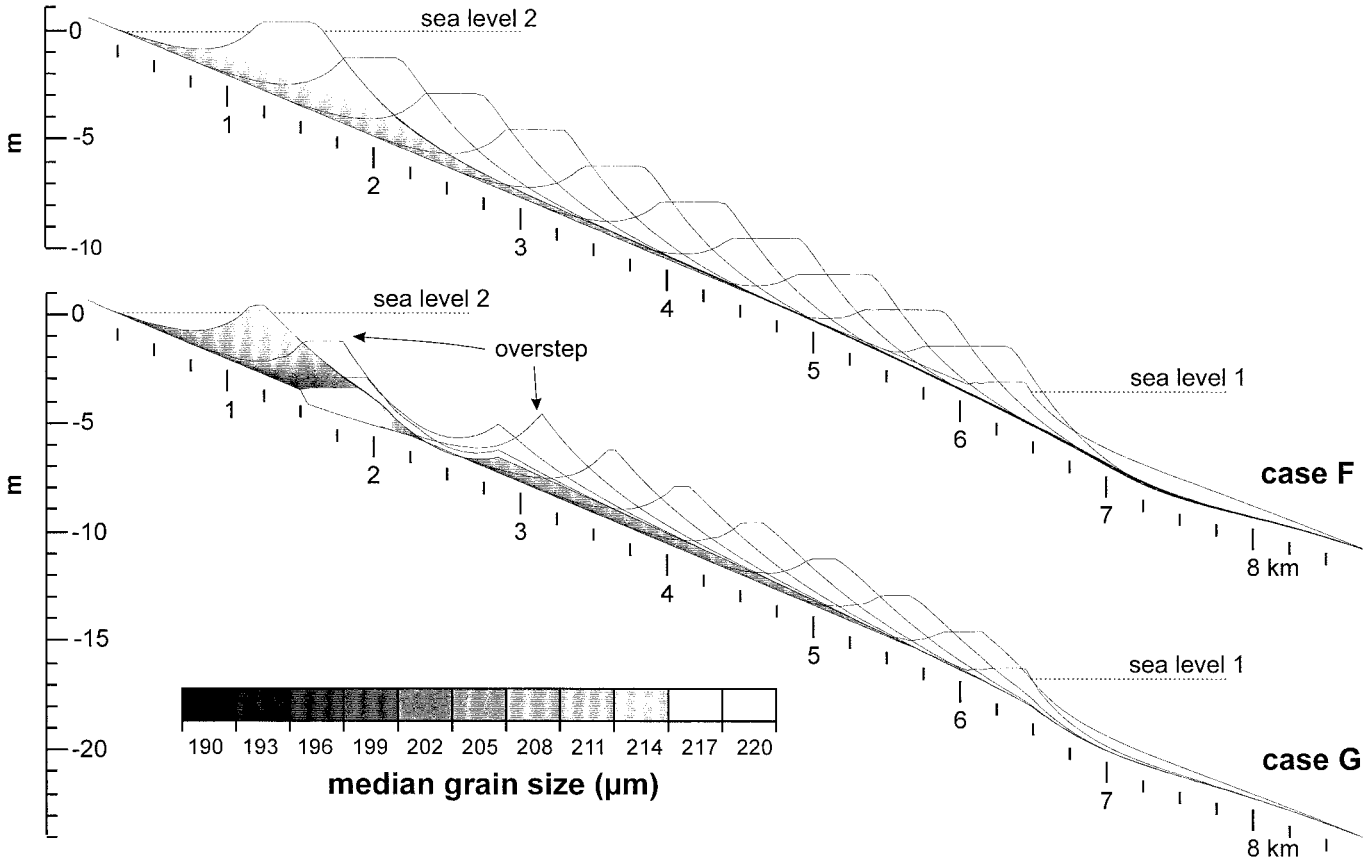

FIG. 15.—Case F shows continuous barrier retreat for a sea-level rise of 825 mm/100 y. Case G shows discontinuous retreat for a sea-level rise of 330 mm/100 y. The total simulated time for case F is 4 times longer (20 ky). The thin lines indicate time-equivalent lines. The horizontal scale is in kilometers; the vertical scale is in meters.

Our model results do not support Rampino and Sanders' (1980) interpretation that barrier overstep results in a characteristic preservation of backbarrier sediments originating from the drowned barrier. After overstepping, the drowned backbarrier deposits are located in shallow water at the shoreface of the newly formed barrier, and the rate and depth of shoreface erosion is sufficient to remove them.

Comparison between Figure 9A and Figure 16 shows that there are similarities between case G and the data of the Caspian Sea regarding the evolution of the barrier system. From 1987 onwards, the width of the Caspian barrier island decreased while the lagoon continued to widen and deepen, which indicates that the system was not in equilibrium. The same effects can be noticed in case G, where a barrier was overstepped at the end of the simulation. This suggests that the Dagestan barrier would have been overstepped if the Caspian Sea level had continued to rise.

Substrate Slope

As described by Roy et al. (1994) and Kaplin and Selivanov (1995), the slope of both the shoreface and shelf is an important variable in coastal morphology. Barrier-type coasts develop only on gentle slopes, whereas steeper slopes give rise to a closed coastline or even cliff formation. In such cases the slope is defined as the submarine slope. The uppermost part

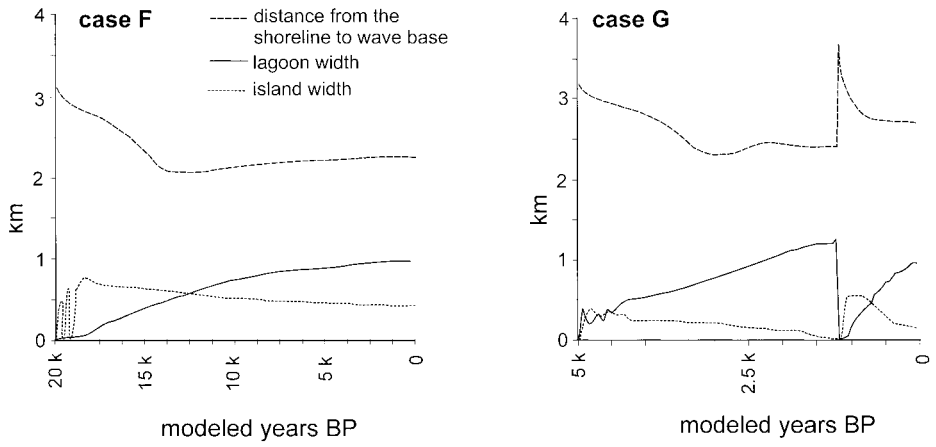

FIG. 16.—Plot showing simulated island width, lagoon width, and distance between wave base and coastline in time for cases F and G. In case F a dynamic equilibrium is reached during transgression in contrast to case G. Here, overstep takes place after about 4 ky. Progradation occurs immediately after barrier overstep as a result of sediment availability through reworking of the overstepped barrier.

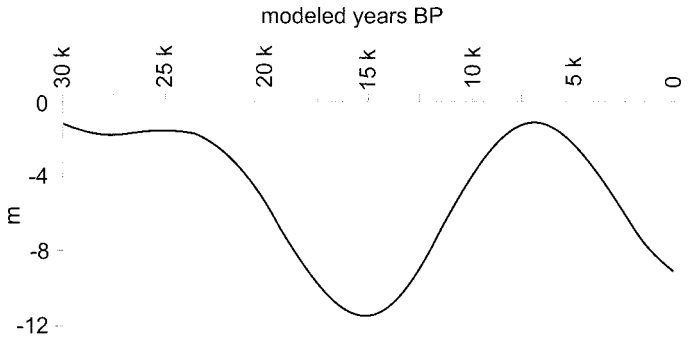

FIG. 17.—Hypothetical relative sea-level curve used as a scenario for cases H and I.

of the submarine slope (middle and upper shoreface) is largely shaped by wave action and does not correspond to the original substrate slope. The influence of waves decreases in an offshore direction, and the original substrate morphology determines the lower part of the submarine slope. The landward side of the coastline (mainland slope) plays a major role during aggradation and retrogradation because it affects the rate of retreat of the mainland–lagoon intersection. We use a straight substrate slope in our simulations in which submarine and subaerial slopes are equal.

Figure 17 shows a hypothetical sea-level curve used as a scenario for two model runs. The resulting simulated stratigraphic records are shown in Figure 18. A constant rate of sediment supply (4 m^2/y) was imposed, and the substrate slope was set to 0.2° for case H and to 0.4° for case I. The substrate slope has two major effects on the model. One is the difference of the rate of retreat of the mainland–lagoon intersection. Under identical rates of sea-level rise, a steep substrate slope results in a slower retreat of the mainland–lagoon intersection compared to a gentle slope. In the former case, the lagoon is much smaller or absent, and there is less accommodation for washover sediments. The greater part of the eroded sediment is thus available for shoreface deposition as opposed to washover sedimentation. A second effect of substrate slope is explained by the fact that the rate of erosion is dependent on water depth whereas the rate of deposition is dependent on the distance to the coastline. The horizontal distance between the storm wave base and the coastline increases with increasing substrate slope. As a result, the relative amount of sediment deposited beyond the wavebase is proportional to substrate slope. Furthermore, sediment deposited beyond the wavebase is relatively coarse grained.

Figure 18A shows the distinct differences between geometry and grain-size distribution for both cases. Stacked sequences of progradational, retrogradational, and progradational deposits can be recognized in both cases. One result of the difference in substrate slope is a change in sedimentation pattern. The dominant sedimentation realm shifts from the backbarrier in case H to the lower shoreface in case I, which partly explains the geometric difference between the two cases. Although the type of sediment used in both cases is identical, the spatial distribution of the grain-size classes is different. In case I, a considerable part of the fine-grained sediments is carried offshore to be deposited beyond the storm-wave base. The absence of this sediment from the total amount of reworkable sediment results in a relative coarsening of the upper to middle shoreface compared to case H.

Substrate slope also affects the internal structure of the sediment body. Figure 18B shows erosion and nondeposition surfaces within the sediment bodies of cases H and I. Case H shows a simple internal structure that reveals a non-depositional transgressive surface where lagoonal deposits rest on subaerially exposed progradational deposits, and a ravinement surface (Swift 1968) that indicates the farthest landward position of the shoreface profile at the end of the transgressive phase. Both surfaces can be recognized in lithologic logs constructed from grain-size trends as the boundaries between individual coarsening-upward cycles. In case H the nondepositional transgressive surface is eroded by the progradational middle shoreface between km 4.0 and 4.5 (see Figure 2B), but this cannot be seen clearly in Figure 18A because the two surfaces are amalgamated. Case I shows a more complex picture. Both progradational sediment bodies reveal an internal erosion surface that separates fine-grained offshore deposits from overlying coarser upper shoreface deposits. This erosion surface is equivalent to the erosion surface of case H which coincides with the maximal transgressive surface between km 4.0 and 4.5. The progradational erosion surfaces are present only in the central part of the progradational deposit, and are absent landward and seaward. All erosional and nondepositional surfaces can be traced in the simulated lithologic logs of Figure 18B, but the lack of continuity of the erosion surfaces in the progradational sequences makes correlation and interpretation between logs difficult.

DISCUSSION

The use of a model as a tool to test ideas causes it to continuously evolve. It will always be subjected to improvements to better mimic reality. The process–response approach described above is no different. The simple numerical model is essentially built around erosion and (shoreface and washover) deposition. The effects of these simulated processes depend on the profile they generate. This feedback creates a dynamic equilibrium between processes and form, and the profile only adapts when necessary. This is an important characteristic of the model because it enables us to simulate complex scenarios that also encompass periods of relative stability in sea level and sediment supply. Our application of the model to real-world data from Terschelling and the Caspian Sea suggests that the simplified representation of erosion and deposition is valid to some extent. The interaction between processes and form generates behavior that has been observed in the real world but that is not explicitly predefined in the model. The slope of the dynamic upper shoreface profile, for example, is dependent on grain size as described by Carter (1988) and Swift (1975). Other examples are the effect of initial substrate slope on coastal morphology, the generation of both erosional and nondepositional boundaries, and continuous versus discontinuous coastal retreat. The model behavior described above makes it potentially useful to critically review some of the concepts put forward by sequence stratigraphy. The absence of behavior rules keeps the model as simple and straightforward as possible.

In the discussion above we have focused on the background of the model and some possible applications. Here we discuss possible extensions or improvements to the model. Compaction due to dewatering of the sediment shortly after deposition is not yet taken into account. The amount of dewatering depends on the initial porosity of the sediment, which is related to the grain-size distribution. Compaction affects the topography and can therefore also affect subsequent coastal behavior. Another improvement to the model would be a reduction in the number of parameters. One example is the parameter for wave efficiency, c_h, which is related to the shape and slope of the upper shoreface and results in variation in the amount of dissipation of wave energy that drives erosion and deposition processes. By coupling upper-shoreface slope and c_h, a better model configuration can be achieved which is updated during runtime. The most important improvement to the model would be to separate storm and fair-weather conditions instead of assuming a time-average storm per timestep. Storms last for a few days, during which time the shoreline is subjected to destructive storm waves resulting in high rates of erosion (Snedden et al. 1988; Morton et al. 1995) and deposition of storm beds offshore (Wiberg 2000). After a storm, a period of recovery and supply of sediment by longshore drift under fair-weather conditions occurs that can last for a long time. These fair-weather periods therefore play an important role in coastal regression. The magnitude and frequency of storm conditions can be described by probability distributions, and the duration of the fair-weather period between two storm events determines the model timestep. These model improvements represent some of our future directions.

The simulated cases described above (A–I) show that process interaction

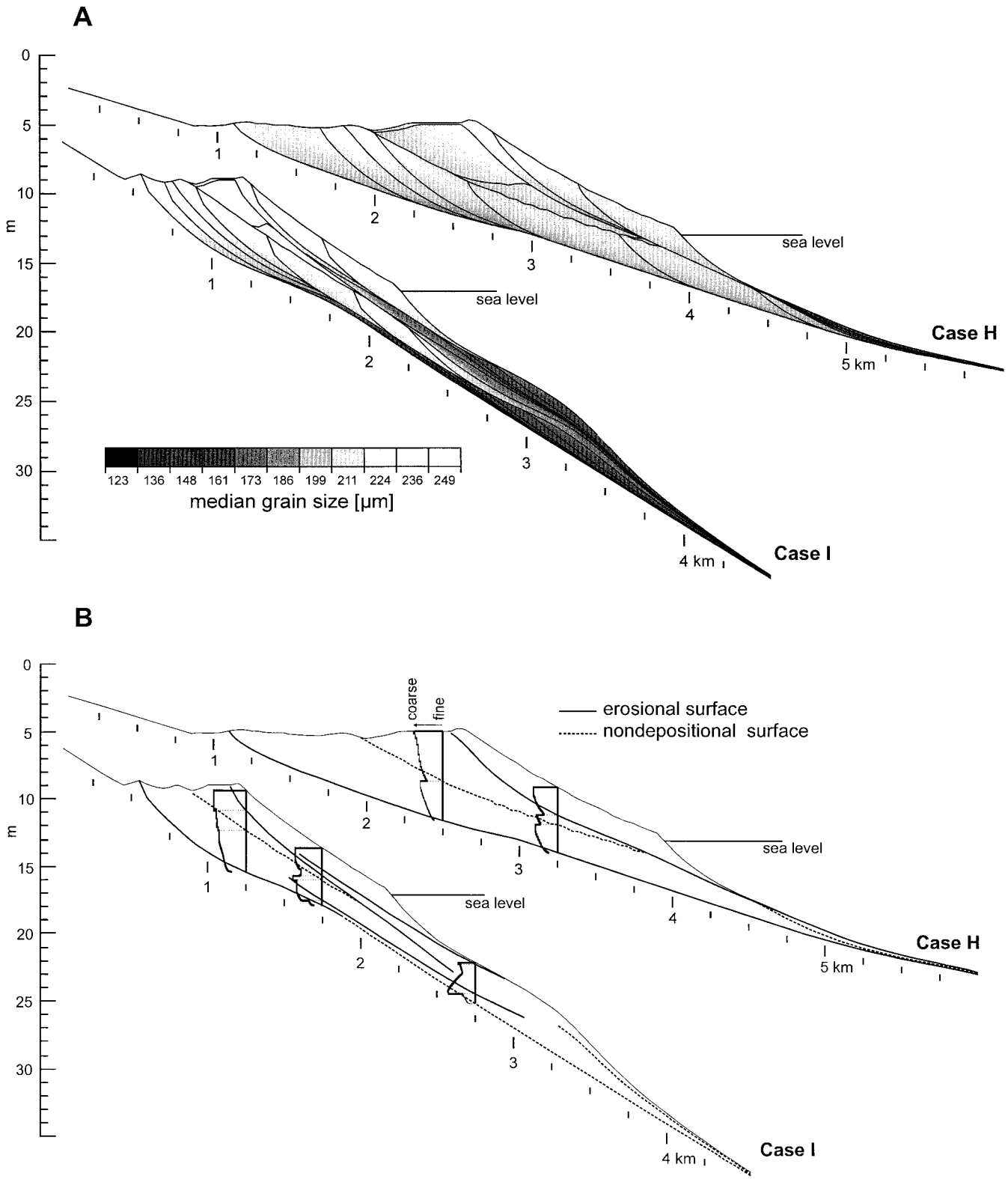

FIG. 18.—**A)** Simulated stratigraphic record based on the sea level shown in Figure 17. Sediment supply is equal in both cases (4 m^2/y). The initial substrate slope for case H is 0.2°, and for case I is 0.4°. The thin lines indicate timelines. The grayscale indicates the mean grain size. **B)** The same stratigraphic record, now indicating erosional and nondeposition surfaces and lithology logs. The horizontal scale is in kilometers, the vertical scale is in meters.

and feedback mechanisms can have unexpected results. Some of these include the effect of initial slope on sorting, progradation after barrier overstepping, effect of initial sediment-size distribution, and generation of erosional and nondepositional surfaces. Although most of these effects will be difficult to confirm in nature, they do suggest that attention should be paid to features that were not considered before. The potential for new insights into the stratigraphic record makes process–response modeling a powerful tool.

CONCLUSIONS

A simple generalization of erosion and deposition can be used to simulate coastal behavior on geologic timescales. There is no need to invoke geometric rules, because feedback between erosion, deposition, and the simulated profile creates a dynamic equilibrium.

The model can be used to evaluate the interaction of sea-level change, rate and type of sediment supply, substrate slope, and wave-base depth.

Transport of multiple grain sizes can be modeled and tuned to actual data on grain-size distributions using sediment travel distances. The relation between travel distance and grain-size class changes with the local wave efficiency, which in turn reflects variation in shoreface slope (dissipation).

Simulated coastal behavior (retrogradation, aggradation, and progradation) and stratigraphy compare well to real-world examples. The rate of sea-level rise determines if retrogradation will be continuous or discontinuous. The initial substrate slope affects the spatial erosion and sedimentation patterns. This results in a variable coastal morphology, geometry of the stratigraphic record, and spatial variation in grain-size distributions.

ACKNOWLEDGMENTS

This research was funded by the DUT-DIOC 3.3 project. NWO (The Netherlands Organization for Scientific Research; grant 047.006.002) and INTAS-EU (grant 94–3382) supported the Caspian fieldwork. We are grateful to Piet Hoekstra and Annika Hesselink, who provided the grain-size data. Thanks are due to Katya Badyukova and Ev. I. Ignatov for providing the Dagestan coast data and discussion on barrier evolution. Furthermore we would like to thank Irina Overeem, Arno Appel, Frank Maartense, and Tim Belser for their comments on earlier versions of the model. The manuscript benefited greatly from useful comments from associate editor Mike Blum and reviewers Daniel Belknap and Donald Swift. The windows-based version of the model is available on request.

REFERENCES

ARPE, K., BENGTSSON, L., GOLITSYN, G.S., MOKHOV, I.I., SEMENOV, V.A., AND SPORYSHEV, P.V., 2000, connection between Caspian Sea level variability and ENSO: Geophysical Research Letters, v. 27, p. 2693–2696.

BRIDGE, J.S., 1981, Hydraulic interpretation of grain-size distributions using a physical model for bedload transport: Journal of Sedimentary Petrology, v. 51, p. 1109–1124.

BRIDGE, J.S., AND BENNETT, S.J., 1992, A model for entrainment and transport of sediment grains of mixed sizes, shapes and densities: Water Resources Research, v. 28, p. 337–363.

BRUUN, P., 1962, Sea level rise as a cause of shore erosion: American Society of Civil Engineers, Proceedings, Journal of the Waterways and Harbors Division, v. 88 (WW1), p. 117–130.

CANT, D.J., 1991, Geometric modeling of facies migration: theoretical development of facies succession and local unconformities: Basin Research, v. 3, p. 51–62.

CARTER, R.W.G., 1988, Coastal Environments—An Introduction to the Physical, Ecological and Cultural Systems of Coastlines: London, Academic Press, 617 p.

COWELL, P.J., ROY, P.S., CLEVERINGA, J., AND DE BOER, P.L., 1999, Simulating coastal systems tracts using the shoreface translation model, *in* Harbaugh, J.W., Watney, W.L., Rankey, E.C., Slingerland, R., Goldstein, R.H., and Franseen, E.K., eds., Numerical Experiments in Stratigraphy: Recent Advances in Stratigraphic and Sedimentologic Computer Simulations: SEPM, Special Publication 62, p. 165–175.

CURRAY, J.R., 1964, Transgression and regression, *in* Miller, R.L., ed., Papers in Marine Geology: New York, The Macmillan Company, p. 175–203.

DAVIS, R.A., JR., 1994, Barrier island systems—a geologic overview, *in* Davis, R.A. Jr., ed., Geology of Holocene Barrier Island Systems: Berlin, Springer-Verlag, p. 1–46.

DAVIS, R.A., JR., AND HAYES, M.O., 1984, What is a wave-dominated coast?: Marine Geology, v. 60, p. 313–329.

DUBOIS, R.N., 1990, Barrier-beach erosion and rising sea level: Geology, v. 18, p. 1150–1152.

FORBES, D.L., SHAW, J., AND TAYLOR, R.B., 1995, Differential preservation of coastal structures on paraglacial shelves: Holocene deposits of Southeastern Canada: Marine Geology, v. 124, p. 187–201.

FORBES, D.L., TAYLOR, R.B., ORFORD, J.D., CARTER, R.W.G., AND SHAW, J., 1991, Gravel barrier migration and overstepping: Marine Geology, v. 97, p. 305–313.

GEORGE, D.J., AND HAND, B.M., 1977, Computer simulation of barrier-island migration: Computers and Geosciences v. 3, p. 469–473.

GUILLÉN, J., AND HOEKSTRA, P., 1996, The ''equilibrium'' distribution of grain size fractions and its implications for cross-shore sediment transport: a conceptual model: Marine Geology, v. 135, p. 15–33.

GUILLÉN, J. AND HOEKSTRA, P., 1997, Sediment distribution in the near shore zone: Grain size evolution in response to shoreface nourishment (Island of Terschelling, the Netherlands): Estuarine, Coastal and Shelf Science, v. 45, p. 639–652.

HARDY, S., AND WALTHAM, D., 1992, Computer modeling of tectonics, eustasy and sedimentation using the Macintosh: Geobyte, v. 7, p. 42–52.

HELLAND-HANSEN, W., AND MARTINSEN, O.J., 1996, Shoreline trajectories and sequences: description of variable depositional-dip scenarios: Journal of Sedimentary Research, v. 66, p. 670–688.

HERON, D.S., JR., MOSLOW, T.F., BERELSON, W.M., HERBERT, J.R., STEELE, G.A., III, AND SUSMAN, K.R., 1984, Holocene sedimentation of a wave-dominated barrier-island shoreline: Cape Lookout, North Carolina: Marine Geology, v. 60, p. 413–434.

KAPLIN, P.A., AND SELIVANOV, A.O., 1995, Recent coastal evolution of the Caspian Sea as a natural model for coastal responses to the possible acceleration of global sea-level rise: Marine Geology, v. 124, p. 161–175.

KAUFMAN, P., GROTZINGER, J.P., AND MCCORMICK, D.S., 1992, Depth-dependent diffusion algorithms for simulation of sedimentation in shallow marine depositional systems, *in* Franseen, E.K., Watney, W.L., Kendall, C.G.St.C., and Ross, W., eds., Sedimentary Modeling; Computer Simulations and Methods for Improved Parameter Definition: Kansas Geological Survey, Special Publication 233, p. 489–508.

KROONENBERG, S.B., BADYUKOVA, E.N. STORMS, J.E.A., IGNATOV, E.I. AND KASIMOV, N.S., 2000, A full sea-level cycle in 65 years: barrier dynamics along Caspian shores: Sedimentary Geology, v. 134, p. 257–274.

LEATHERMAN, S.P., 1983, Barrier island evolution in response to sea level rise: a discussion: Journal of Sedimentary Petrology, v. 53, p. 1026–1031.

LEATHERMAN. S.P., AND WILLIAMS, A.T., 1983, Vertical sedimentation units in a barrier island washover fan: Earth Surface Processes and Landforms, v. 8, p. 141–150.

MORTON, R.A., GIBEAUT, J.C., AND PAINE, J.G., 1995, Meso-scale transfer of sand during and after storms: implications for prediction of shoreline movement: Marine Geology, v. 126, p. 161–179.

NIEDORODA, A.W., REED, C.W., SWIFT, D.J.P., ARATO, H., AND HOYANAGI, K., 1995, Modeling shore-normal large-scale coastal evolution: Marine Geology, v. 126, p. 181–199.

NUMMEDAL, D., RILEY, G.W., AND TEMPLET, P.L., 1993a, High-resolution sequence architecture: a chronostratigraphic model based on equilibrium profile studies, *in* Posamentier, H.W., Summerhayes, C.P., Haq, B.U., and Allen, G.P., eds., Sequence Stratigraphy and Facies Associations: International Association of Sedimentologists, Special Publication 18, p. 55–68.

NUMMEDAL, D., WOLTER, N.R., FLEMMING, T.F., BERGSOHN, I., AND SWIFT, D.J.P., 1993b, Lowstand, shallow marine sandstones in upper Cretaceous strata of the San Juan basin, New Mexico, *in* Caldwell, W.G.E., and Kauffman, E.G., eds., Evolution of the Western Interior Basin: Geological Association of Canada, Special Paper 39, p. 199–218.

PENLAND, S., SUTER, J.R., AND BOYD, R., 1985, Barrier island arcs along abandoned Mississippi River deltas: Marine Geology, v. 63, p. 197–233.

PILKEY, O.H., AND DAVIS, T.W., 1987, An analysis of coastal recession models: North Carolina coast, *in* Nummedal D., Pilkey O.H., Howard J.D., and Price, W.A., eds., Sea-Level Fluctuation and Coastal Evolution: SEPM, Special Publication 41, p. 59–68.

PLINT, A.G., 1988, Sharp-based shoreface sequences and ''offshore bars'' in the Cardium Formation of Alberta: their relationship to relative changes in sea level, *in* Wilgus, C.K., Hastings, B.S., Kendall, C.G.St.C., Posamentier, H.W., Ross, C.A., and Van Wagoner, J.C., eds., Sea-Level Changes—An Integrated Approach: SEPM, Special Publication 42, p. 357–370.

POLONSKI, V.F., MIKHAYLOV, V.N., AND KIR'YANOV, S.V., 1998, The Volga River mouth area: Hydrological–morphological processes, regime of contaminants and influence of the Caspian Sea level changes: Moscow, GEOS, 280 p. (in Russian).

POSAMENTIER, H.W., ALLEN, G.P., JAMES, D.P., AND TESSON, M., 1992, Forced regressions in a sequence stratigraphic framework: concepts, examples, and exploration significance: American Association of Petroleum Geologists, Bulletin, v. 76, p. 1687–1709.

RAMPINO, M.R., AND SANDERS, J.E., 1980, Holocene transgression in south-central Long Island, New York: Journal of Sedimentary Petrology, v. 50, p. 1063–1080.

RAMPINO, M.R., AND SANDERS, J.E., 1982, Holocene transgression in south-central Long Island, New York—Reply: Journal of Sedimentary Petrology, v. 53, p. 1020–1025.

RAMPINO, M.R., AND SANDERS, J.E., 1983, Barrier island evolution in response to sea level rise: reply: Journal of Sedimentary Petrology, v. 53, p. 1031–1033.

RODIONOV, S., 1994, Global and Regional Climate Interaction; The Caspian Sea Experience: Dordrecht, The Netherlands, Kluwer, p. 241.

ROY, P.S., COWELL, P.J., FERLAND, M.A., AND THOM, B.G., 1994, Wave dominated coasts, *in* Carter, R.W.G., and Woodroffe, C.D., eds., Coastal Evolution—Late Quaternary Shoreline Morphodynamics, Cambridge, U.K., Cambridge University Press, p. 121–186.

SNEDDEN, J.W., NUMMEDAL, D., AND AMOS, A.F., 1988, Storm- and fair-weather combined flow on the central Texas continental shelf: Journal of Sedimentary Petrology, v. 58, p. 580–595.

STECKLER, M., 1999, High-resolution sequence stratigraphic modeling 1: The interplay of sedimentation, erosion, and subsidence, *in* Harbaugh, J.W., Watney, W.L., Rankey, E.C., Slingerland, R., Goldstein, R.H., and Franseen, E.K., eds., Numerical Experiments in Stratigraphy: Recent Advances in Stratigraphic and Sedimentologic Computer Simulations: SEPM, Special Publication 62, p. 139–149.

STIVE, M.J.F., AND DE VRIEND, H.J., 1995, Modeling shoreface profile evolution: Marine Geology, v. 126, p. 235–248

STORMS, J.E.A., WELTJE, G.J., VAN DIJKE, J.J., AND KROONENBERG, S.B., 1999, 2D process response modeling of shoreface evolution and barrier island behaviour on geological timescales, *in* Lippard S.J., Næs A., and Sinding-Larsen R., eds., Proceedings of the International Association for Mathematical Geology, Trondheim, Norway, p. 563–568.

SWIFT, D.J.P., 1968, Coastal erosion and transgressive stratigraphy: Journal of Geology, v. 76, p. 444–456.

SWIFT, D.J.P., 1975, Barrier-island genesis: evidence from the central Atlantic shelf, eastern U.S.A.: Sedimentary Geology, v. 14, p. 1–43.

SWIFT, D.J.P. AND MOSLOW, T.F., 1982, Holocene transgression in south-central Long Island, New York—Discussion: Journal of Sedimentary Petrology, v. 53, p. 1014–1019.

SWIFT, D.J.P., PHILLIPS, S., AND THORNE, J.A., 1991, Sedimentation on continental margins, IV: lithofacies and depositional systems, *in* Swift, D.J.P., Oertel, G.G., Tillman, R.W., and Thorne, J.A., eds., Shelf Sand and Sandstone Bodies: International Association of Sedimentologists, Special Publication 14, p. 89–152.

SWIFT, D.J.P., AND THORNE, J.A., 1991, Sedimentation on continental margins, I: A general model for shelf sedimentation, *in* Swift, D.J.P., Oertel, G.G., Tillman, R.W., and Thorne, J.A., eds., Shelf Sand and Sandstone Bodies: International Association of Sedimentologists, Special Publication 14, p. 3–31.

THOM, B.G., 1983, Transgressive and regressive stratigraphies of coastal sand barriers in Southeast Australia: Marine Geology, v. 56, p. 137–158.

WIBERG, P., 2000, A perfect storm: formation and potential for preservation of storm beds on the continental shelf: Oceanography, v. 13, p. 93–99.

WRIGHT, L.D., AND SHORT, A.D., 1983, Morphodynamics of beaches and surfzones in Australia, *in* P.D. Komar, ed., CRC Handbook of Coastal Processes and Erosion: Boca Raton, Florida, CRC Press, p. 35–64.

Received 22 March 2000; accepted 25 May 2001.